

# Control and Synchronization of Fractional-Order Chaotic Systems

Ahmed G. Radwan, Wafaa S. Sayed and Salwa K. Abd-El-Hafiz

**Abstract** The chaotic dynamics of fractional-order systems and their applications in secure communication have gained the attention of many recent researches. Fractional-order systems provide extra degrees of freedom and control capability with integer-order differential equations as special cases. Synchronization is a necessary function in any communication system and is rather hard to be achieved for chaotic signals that are ideally aperiodic. This chapter provides a general scheme of control, switching and generalized synchronization of fractional-order chaotic systems. Several systems are used as examples for demonstrating the required mathematical analysis and simulation results validating it. The non-standard finite difference method, which is suitable for fractional-order chaotic systems, is used to solve each system and get the responses. Effect of the fractional-order parameter on the responses of the systems extended to fractional-order domain is considered. A control and switching synchronization technique is proposed that uses switching parameters to decide the role of each system as a master or slave. A generalized scheme for synchronizing a fractional-order chaotic system with another one or with a linear combination of two other fractional-order chaotic systems is presented. Static (time-independent) and dynamic (time-dependent) synchronization, which could generate multiple scaled versions of the response, are discussed.

**Keywords** Active nonlinear control • Amplitude modulation • Hidden attractors • Lyapunov stability • Non-standard finite difference schemes • Static and dynamic synchronization

---

A.G. Radwan (✉) · W.S. Sayed · S.K. Abd-El-Hafiz  
Faculty of Engineering, Engineering Mathematics and Physics Department,  
Cairo University, Giza 12613, Egypt  
e-mail: agradwan@ieee.org

W.S. Sayed  
e-mail: wafaa.s.sayed@eng.cu.edu.eg

S.K. Abd-El-Hafiz  
e-mail: salwa@computer.org

A.G. Radwan  
Nanoelectronics Integrated Systems Center, Nile University, Cairo 12588, Egypt

## 1 Introduction

Chaotic systems and their implementations have been studied heavily during the last four decades [41, 42, 45, 50, 80]. The sensitivity of chaotic systems to parameters and initial conditions is required for many applications such as chemical reactions [18], biological systems [33, 67], circuit theory [40, 46, 51, 52], electronics [62], control [4, 5], secure communication [14, 16, 27] and cryptography [1, 2, 6, 26, 47, 48, 56, 58–60]. Much attention has been devoted to the search for better and more efficient methods for obtaining the analytical or numerical solutions or controlling the responses of chaotic systems. During the last few decades, fractional calculus has also become a powerful tool in describing the dynamics of complex systems which appear frequently in several branches of science and engineering. Therefore, fractional differential equations and their numerical techniques find numerous applications in the field of viscoelasticity, robotics, feedback amplifiers, electrical circuits, control theory, electro analytical chemistry, fractional multi-poles, electromagnetics, bioengineering, and image encryption [10, 17, 30, 39, 49, 54, 55, 57, 63, 64].

The chaotic dynamics of fractional-order systems began to attract the interest of the scientific community in recent years associated with the advances in numerical methods for solving fractional-order systems and their electronic implementations [10]. In addition, fractional calculus is more suitable for modeling the continuous non-standard behaviors of nature due to the flexibility offered by the extra degrees of freedom. Recently, most of the chaotic dynamical systems based on integer-order calculus have been extended into the fractional-order domain to fit the experimental data much precisely than the integer-order modeling.

The coupling of two or more chaotic systems is referred to as synchronization. Control and synchronization of fractional-order chaotic systems have found their way to many applications such as biological and physical systems, structural engineering, ecological models, secure communication and cryptography [3, 7–9, 11, 12, 15, 22, 35, 36, 66, 76, 79]. Since the introduction of the concept of synchronization of two chaotic signals starting at different initial conditions [38], there has been a lot of work on chaos control and synchronization. Chaotic synchronization represents a challenge due to the sensitivity to initial conditions characteristic of chaotic systems. Two trajectories starting at slightly different initial conditions exponentially diverge from each other in the long-term evolution. Several papers handled conventional synchronization of two identical chaotic systems, their anti-synchronization [21], as well as synchronization of two different systems [77]. More recent researches extended the concept to fractional-order domain [33], introduced generalized scaled dynamic (time-dependent) synchronization [43, 61], and provided the capability of control and switching for exchanging roles between master and slave systems [19, 44].

The aim of this chapter is to introduce several methods for control and synchronization of fractional-order chaotic systems using active nonlinear control technique. Several chaotic systems are extended to fractional-order domain and the effect of the

fractional-order parameter on the output responses is studied. The concept of active control using two on/off switches for the synchronization between two fractional-order chaotic systems is proposed. A generalized synchronization scheme is applied to synchronize two identical or different fractional-order chaotic systems. In addition, a new chaotic system is formed as a linear combination of two systems where the generalized synchronization scheme is applied to synchronize a system with the linear combination of two other systems. A block diagram of the generalized synchronization scheme and the associated mathematical analysis are presented. The control signals are obtained in terms of the responses, parameters and scaling factors. Generalizations permit conventional synchronization, anti-synchronization, static scaling, as well as dynamic scaling where the type of synchronization and the scaling factor vary as time advances. Mathematical analysis and various examples are presented at different values of fractional-orders using Grünwald-Letnikov method of approximation and Non-Standard Finite Difference (NSFD) discretization technique [24]. Simulation results, including time series and strange attractors, are consistent with the performed analysis.

Section 2 of this chapter provides a brief introduction to relevant concepts and a survey of previous works on control and synchronization of chaotic dynamics. Section 3 provides the preliminaries of numerical solution of fractional-order differential equations and reviews the properties of the systems chosen for numerical simulations. Section 4 illustrates the effect of parameters and fractional-orders on the responses of the utilized chaotic systems. Section 5 presents active nonlinear control and synchronization using two on/off switches for the synchronization between two different chaotic systems. Section 6 discusses the analysis required to get the control signals, which is suitable for achieving any required synchronization case. This analysis is validated through simulation results for two identical or different fractional-order chaotic systems. Section 7 proposes analysis and simulation results in case of synchronizing a fractional-order chaotic system with a linear combination of two other systems. In addition, results show that the linear combination provides another way of controlling the obtained attractor diagram. Finally, Sect. 8 summarizes the main contributions of the chapter.

## 2 Control and Synchronization of Chaotic Dynamics

System parameters and fractional-orders represent a way of controlling the type of obtained response with no external control procedure. Chaos control requirements differ according to the given specifications and application. It is sometimes required to stabilize the system and force it to follow a certain periodic solution, while other cases require conservative systems with quasi-periodic solutions. Other modeling applications as well as pseudo-random number generation and utilization in cryptography require chaotic responses.

Continuous flows expressed in terms of ordinary differential equations can have numerous types of post transient solution(s). Reporting when these systems of differential equations exhibit chaos represents a rich research field. Research efforts have been exerted (e.g., [25, 65]) to come up with simple novel chaotic flows other than the well-known conventional systems (Lorenz, Rössler, ...). These researches depend on Poincaré-Bendixson theorem, [20] which states that for any autonomous first-order ordinary differential equations with continuous functions to have chaotic solutions it requires at least three dimensions with at least one nonlinear term. Some systematic numerical search methods have been developed for detecting the presence of chaotic solutions for new equations that contain multiple parameters. These parameters mainly appear as the coefficients of each term in the system of differential equations. Methods aim at setting many coefficients to zero with the others set to  $\pm 1$  if possible or otherwise to a small integer or decimal fraction with the fewest possible digits. These systems, with the least number of existing coefficients and nonlinear terms, should exhibit chaotic properties of aperiodic bounded long-time evolution and sensitive dependence on initial conditions for some ranges of parameters.

Continuous chaotic systems can be classified into two wide categories. Dissipative systems, to which most of the studied systems belong, usually exhibit chaos for most initial conditions in a specified range of parameters. On the other hand, a conservative system exhibits periodic and quasi-periodic solutions for most values of parameters and initial conditions, and can exhibit chaos for special values only. Consequently, dissipative systems usually appear in most applications of chaos theory such as chaos-based communication, physical and financial modeling. It should be noted that conservative systems have another different set of applications where they are useful to study the development of chaos in some kinds of systems.

Another important classification of chaotic or strange attractors is either self-excited or hidden attractors. A self-excited attractor has a basin of attraction that is associated with or excited from unstable equilibria. For example, the well-known Lorenz and Rössler attractors are self-excited. From a computational point of view, this allows one to use a numerical method in which a trajectory started from a point, on the unstable manifold in the neighborhood of an unstable equilibrium, reaches an attractor and identifies it. On the other hand, a hidden attractor has a basin of attraction that does not intersect with small neighborhoods of any equilibrium points. Hidden attractors cannot be found by the previous method and are important in engineering applications because they allow unexpected and potentially disastrous responses to perturbations in a structure like a bridge or an airplane wing.

As for external control methods, Pecora and Carroll [38] were the first to introduce the concept of synchronization of two systems with different initial conditions. Many chaotic synchronization schemes have also been introduced during the last decade such as adaptive control [68–73], time delay feedback approach [13, 37], sliding mode control [11, 23], nonlinear feedback synchronization, and active control [22]. However, most of these methods have been tested for two identical chaotic systems. When Ho and Hung [22] presented and applied the concept of active control method on the synchronization of chaotic systems, many recent papers investigated this technique for different systems and in different applications [28, 74].

The synchronization of three chaotic fractional-order Lorenz systems with bidirectional coupling in addition to the chaos synchronization of two identical systems via linear control were investigated in [34, 78]. Moreover, two different fractional-order chaotic systems can be synchronized using active control as in [7]. The hyper-chaotic synchronization of the fractional-order Rössler system, which exists when its order is as low as 3.8, was shown by Yua and Lib [78].

Anti-synchronization is a phenomenon in which the state vectors of the synchronized systems have the same amplitude but opposite signs to those of the driving system. Therefore, the sum of two signals is expected to converge to zero when anti-synchronization appears. Since the discovery of anti-synchronization experimentally in the context of self-synchronization, it has been applied in many different fields, such as biological and physical systems, structural engineering, and ecological models [75]. Liu et al. [29] shows that either synchronization or anti-synchronization can appear depending on the initial conditions of the coupled pendula. Active control method is used to study the anti-synchronization for two identical and nonidentical systems [7, 22].

Before we proceed to presenting our work on control and synchronization of fractional-order chaotic systems, the numerical methods associated with fractional-order differential equations are briefly reviewed in the next section.

### 3 Fractional-Order Chaotic Systems and Their Numerical Solution

Finding robust and stable numerical and analytical methods for solving the fractional differential equations has recently been an active research topic. These methods include the fractional difference method, the Adomian decomposition method, the homotopy-perturbation method, the variational iteration method, and the Adams-Bashforth-Moulton method. Recently, the non-standard finite difference (NSFD) scheme [31, 32] has been applied for the numerical solutions of fractional differential equations [24]. The scheme has been developed as an alternative method for solving a wide range of problems whose mathematical models involve algebraic, differential, biological models, and chaotic systems. The definition of Grünwald-Letnikov derivative has been used in numerical analysis to discretize the fractional differential equations. The technique has many advantages over the classical techniques, and provides an efficient numerical solution.

The Caputo fractional derivative [17] of order  $\alpha$  is defined as:

$$D^\alpha f(t) = \frac{d^\alpha f(t)}{dt^\alpha} = \begin{cases} \frac{1}{\Gamma(m-\alpha)} \int_0^t \frac{f^m(\tau)}{(t-\tau)^{\alpha-m+1}} d\tau & m-1 < \alpha < m \\ \frac{d^m}{dt^m} f(t) & \alpha = m \end{cases}, \quad (1)$$

where  $m$  is the first integer greater than  $\alpha$  and  $\Gamma(\cdot)$  is the gamma function defined by:

$$\Gamma(z) = \int_0^\infty e^{-t} t^{z-1} dt, \quad \Gamma(z + 1) = z\Gamma(z). \tag{2}$$

Consider the fractional-order differential equation

$$D^\alpha x(t) = f(t, x). \tag{3}$$

Grünwald-Letnikov method of approximation [24] is defined as follows:

$$D^\alpha x(t) = \lim_{h \rightarrow 0} h^{-\alpha} \sum_{j=0}^{t/h} (-1)^j \binom{\alpha}{j} x(t - jh), \tag{4}$$

where  $h$  is the step size. This equation can be discretized as follows:

$$\sum_{j=0}^{n+1} c_j^\alpha x(t - jh) = f(t_n, x(t_n)), \quad j = 1, 2, 3, \dots \tag{5}$$

where  $t_n = nh$  and  $c_j^\alpha$  are the Grünwald-Letnikov coefficients defined as:

$$c_j^\alpha = \left(1 - \frac{1 + \alpha}{j}\right) c_{j-1}^\alpha, \quad j = 1, 2, 3, \dots, \quad c_0^\alpha = h^{-\alpha}. \tag{6}$$

The NSFD discretization technique is based on replacing the step size  $h$  by a function  $\phi(h)$  [24, 33] and applying it with (5) to solve (3). In the rest of this paper, NSFD with  $\phi(h) = 1 - e^{-h}$  is used to solve the systems of differential equations. In addition, a time step of 0.005 is employed according to the system properties and a total simulation time of 200 points is used except where stated otherwise.

Same algebraic manipulation can be applied to a system of three fractional-order differential equations

$$D^\alpha x = f_1(x, y, z), \tag{7a}$$

$$D^\beta y = f_2(x, y, z), \tag{7b}$$

$$D^\gamma z = f_3(x, y, z), \tag{7c}$$

where  $0 < \alpha, \beta, \gamma \leq 1$ , to obtain the corresponding solutions. All state variables ( $x, y, z, \dots$ ), scaling factors ( $s_x, s_y, s_z, \dots$ ), and control functions ( $u_x, u_y, u_z, \dots$ ) that will appear later on are in general functions of time, i.e., their values may change at every time instant.

### 3.1 Systems Utilized for Synchronization Purposes

The first three systems are Lü, Newton-Leipnik and Chua’s circuit, which have appeared before in fractional-order form in [39, 53] and others. The rest of the utilized systems appeared before in integer-order [25, 65], yet, in this section, they are extended to fractional-order domain. One of the systems is the slave, while the master may be one of the other two systems or a linear combination of them as detailed later on in Sect. 7. Table 1 shows the equations of the selected systems in fractional-order domain and their strange attractors in the integer-order case. They are a dissipative

**Table 1** Equations of the utilized systems, their properties, discretized solutions and attractor diagrams

System	Lü system [39]	Newton-Leipnik [39]	Chua’s circuit [53]
Equations	$D^\alpha x = a(y-x)$ $D^\beta y = -xz + by$ $D^\gamma z = xy - cz$	$D^\alpha x = -ax + y + 10yz$ $D^\beta y = -x - 0.4y + 5xz$ $D^\gamma z = -5xy + bz$	$D^\alpha x = a(y-f(w)x)$ $D^\beta y = z - x$ $D^\gamma z = -by + cz$ $Dw = x$ , where $f(w) = \begin{cases} a, &  w  < 1 \\ e, &  w  \geq 1 \end{cases}$
Parameters	$(a, b, c) = (36, 20, 3)$	$(a, b) = (0.4, 0.175)$	$(a, b, c, d, e) = (4, 1, 0.65, 0.2, 5)$
Initial Point	$(x_0, y_0, z_0) = (0.2, 0.5, 0.3)$	$(x_0, y_0, z_0) = (0.19, 0, -0.18)$	$(x_0, y_0, z_0, w_0) = (0.01, 0.02, 0.01, 0.05)$
Discretized Solution	$x_{n+1} = \frac{-\sum_{j=1}^{n+1} e^{j\alpha} x_{n+1-j} + ay_n - ax_n}{c_0^\alpha}$ $y_{n+1} = \frac{-\sum_{j=1}^{n+1} e^{j\beta} y_{n+1-j} - x_n + 15n + by_n}{c_0^\beta}$ $z_{n+1} = \frac{-\sum_{j=1}^{n+1} e^{j\gamma} z_{n+1-j} + x_{n+1} 5n + 1 - cz_n}{c_0^\gamma}$	$x_{n+1} = \frac{-\sum_{j=1}^{n+1} e^{j\alpha} x_{n+1-j} - ax_n + y_n + 10y_n z_n}{c_0^\alpha}$ $y_{n+1} = \frac{-\sum_{j=1}^{n+1} e^{j\beta} y_{n+1-j} - x_{n+1} - 0.4y_n + 5x_{n+1} 5n}{c_0^\beta}$ $z_{n+1} = \frac{-\sum_{j=1}^{n+1} e^{j\gamma} z_{n+1-j} - 5x_{n+1} 5n + 1 + bz_n}{c_0^\gamma}$	$x_{n+1} = \frac{-\sum_{j=1}^{n+1} e^{j\alpha} x_{n+1-j} + ay_n - af(w)z_n}{c_0^\alpha}$ $y_{n+1} = \frac{-\sum_{j=1}^{n+1} e^{j\beta} y_{n+1-j} + z_n - x_{n+1}}{c_0^\beta}$ $z_{n+1} = \frac{-\sum_{j=1}^{n+1} e^{j\gamma} z_{n+1-j} - by_{n+1} + cz_n}{c_0^\gamma}$ $w_{n+1} = w_n + hx_n$
Attractor	$\alpha = 1$ $\beta = 1$ $\gamma = 1$		
System	A dissipative hidden attractor [25]	A dissipative self-excited attractor [65]	A conservative system [25]
Equations	$D^\alpha x = -y$ $D^\beta y = x + z$ $D^\gamma z = 2y^2 + xz - a$	$D^\alpha x = y$ $D^\beta y = z$ $D^\gamma z = -y - az + b\left(\frac{z}{c} - c\right)$	$D^\alpha x = y$ $D^\beta y = -x - zy$ $D^\gamma z = y^2 - a$
Parameters	$a = 0.35$	$(a, b, c) = (0.6, 0.58, 1)$	$a = 1$
Initial Point	$(x_0, y_0, z_0) = (0, 0.4, 1)$	$(x_0, y_0, z_0) = (0.25, 0.2, 0.25)$	$(x_0, y_0, z_0) = (0, 5, 0)$
Discretized Solution	$x_{n+1} = \frac{-\sum_{j=1}^{n+1} e^{j\alpha} x_{n+1-j} - y_n}{c_0^\alpha}$ $y_{n+1} = \frac{-\sum_{j=1}^{n+1} e^{j\beta} y_{n+1-j} + x_n + z_n}{c_0^\beta}$ $z_{n+1} = \frac{-\sum_{j=1}^{n+1} e^{j\gamma} z_{n+1-j} + 2y_n^2 + x_{n+1} z_n - a}{c_0^\gamma + x_{n+1}}$	$x_{n+1} = \frac{-\sum_{j=1}^{n+1} e^{j\alpha} x_{n+1-j} + y_n}{c_0^\alpha}$ $y_{n+1} = \frac{-\sum_{j=1}^{n+1} e^{j\beta} y_{n+1-j} + z_n}{c_0^\beta}$ $z_{n+1} = \frac{-\sum_{j=1}^{n+1} e^{j\gamma} z_{n+1-j} - y_{n+1} - az_n + b\left(\frac{z_n + 1}{c} - c\right)}{c_0^\gamma}$	$x_{n+1} = \frac{-\sum_{j=1}^{n+1} e^{j\alpha} x_{n+1-j} + y_n}{c_0^\alpha}$ $y_{n+1} = \frac{-\sum_{j=1}^{n+1} e^{j\beta} y_{n+1-j} - x_{n+1} - 2zy_n}{c_0^\beta - z_n}$ $z_{n+1} = \frac{-\sum_{j=1}^{n+1} e^{j\gamma} z_{n+1-j} + y_{n+1}^2 - a}{c_0^\gamma}$
Attractor	$\alpha = 1$ $\beta = 1$ $\gamma = 1$		

hidden attractor with no equilibria and quadratic non-linearity [25], a dissipative self-excited attractor with quadratic non-linearity [65], and a conservative one [25] with the equations shown in Table 1.

Discretized solutions to the systems could be obtained using (5) and NSFD. Non-linear terms including the same state variable that is being calculated are replaced with the aid of the nonlocal discrete representations. For example, in the equation of  $D^\beta y$ , the following rules are used for replacement:

$$y \approx y_n \quad y^2 \approx y_n y_{n+1}, \quad xy \approx 2x_{n+1}y_n - x_{n+1}y_{n+1}, \quad \text{and} \quad zy \approx 2z_n y_n - z_n y_{n+1}. \quad (8)$$

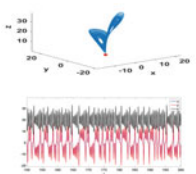
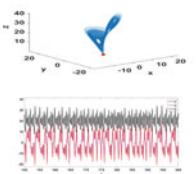
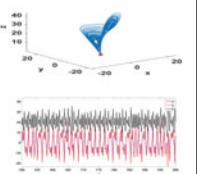
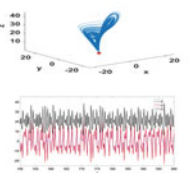
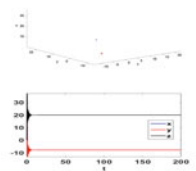
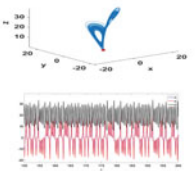
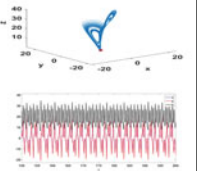
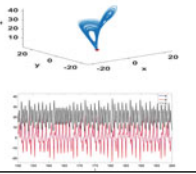
The relations used for solving the systems are given in Table 1.

Subscripts will be used later on to characterize different roles that a system could act as a master or slave. There are various possible values for the fractional-orders where the effect of fractional-orders and criteria of choosing them are studied in the next section.

### 4 Sensitivity to Fractional-Orders and Parameters Variation

In this section, we discuss the sensitivity of the six presented systems to parameters and fractional-orders. Numerical simulations are used to identify when they generate periodic or chaotic responses. In addition, we compare the shape of their attractors in integer-order and fractional-order. For simplicity, the three fractional-orders in

**Table 2** Lü system responses versus fractional-order  $\alpha$  and parameter  $a$

	$\alpha = 0.92$	$\alpha = 0.95$	$\alpha = 0.98$	$\alpha = 1$
$a = 30$	Chaotic 	Chaotic 	Chaotic 	Chaotic 
$a = 36$	Stable 	Chaotic 	Chaotic 	Chaotic 



**Table 3** Newton-Leipnik system responses versus fractional-order  $\alpha$  and parameters

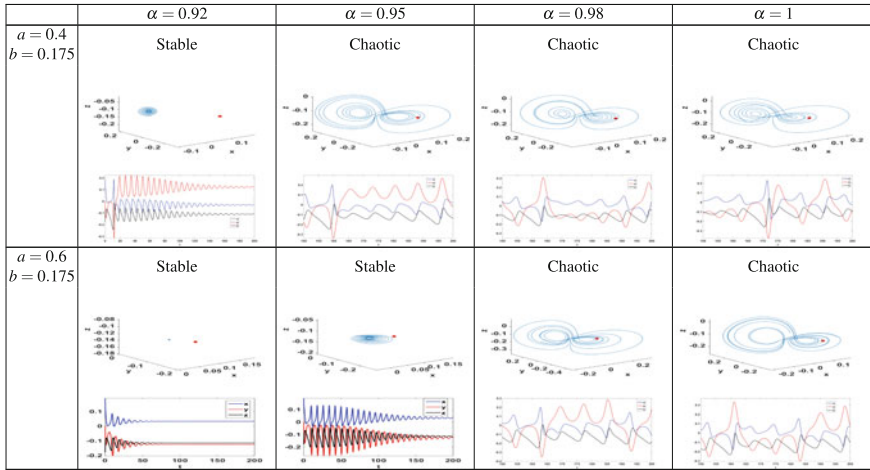
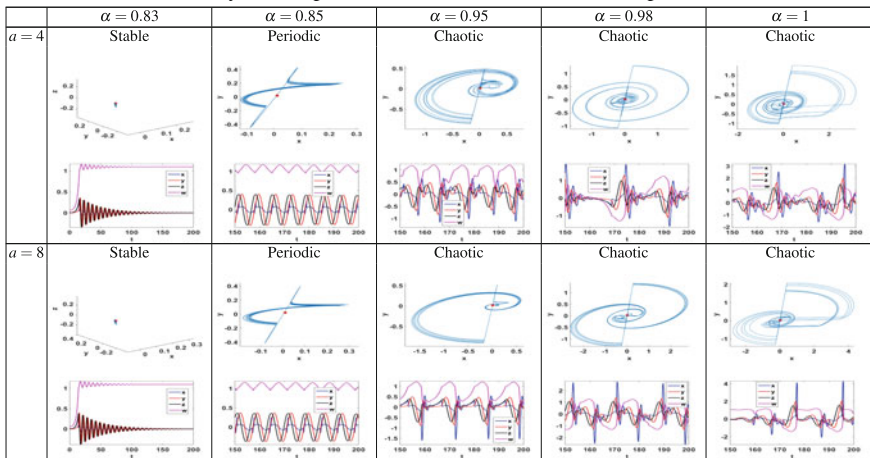


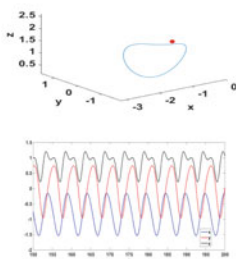
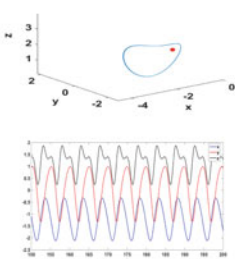
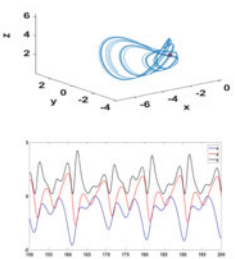
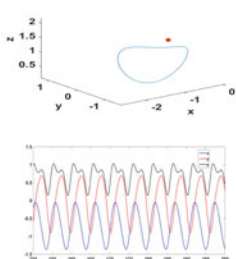
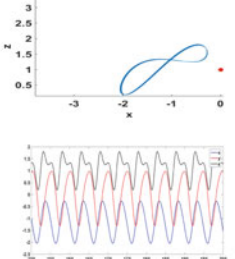
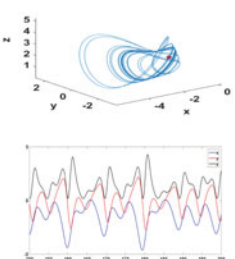
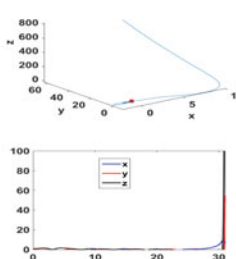
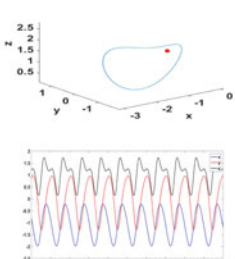
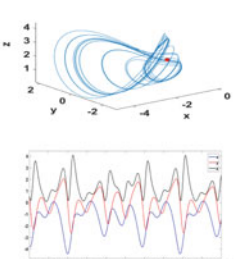
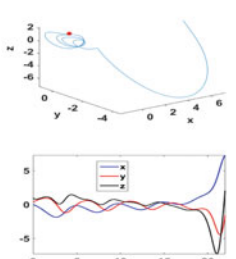
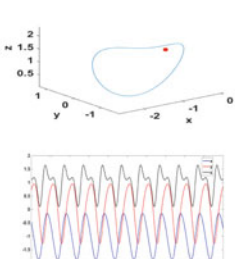
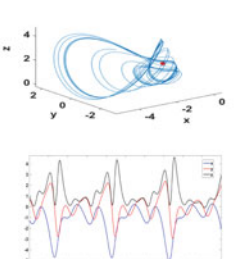
**Table 4** Chua's circuit system responses versus fractional-order  $\alpha$  and parameter  $a$



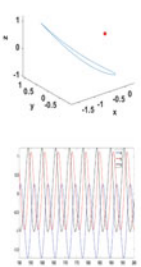
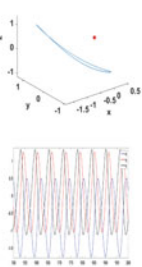
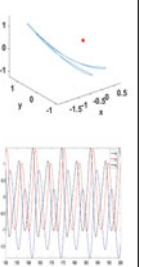
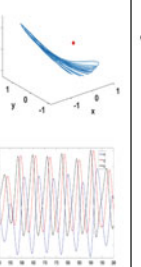
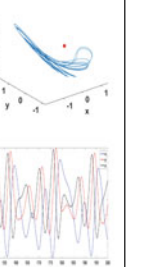
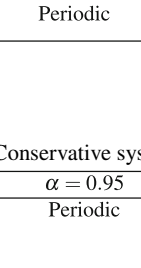
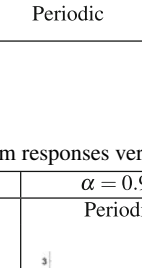
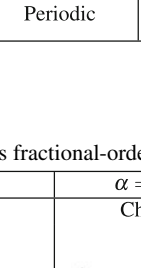
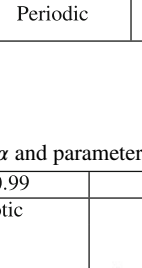
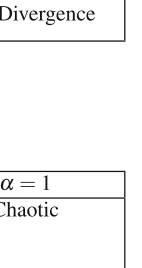
the system of fractional differential equations are assumed to be equal, i.e., in this section  $\alpha = \beta = \gamma$  and the unified fractional-order is denoted by  $\alpha$ .

Tables 2, 3, 4, 5, 6 and 7 show the post-transient time series of the 3 phase space dimensions  $x, y$  and  $z$  as well as the post-transient attractor diagram with the initial point marked in red illustrating the obtained type of solution (periodic or chaotic) for different values of the fractional-order. It should be noted that in the upcoming

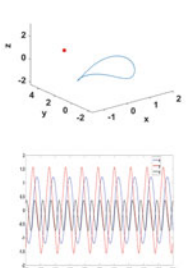
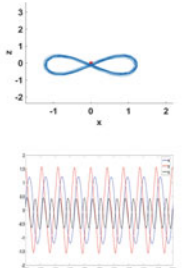
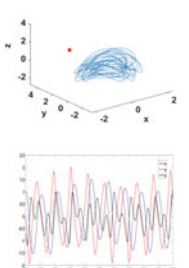
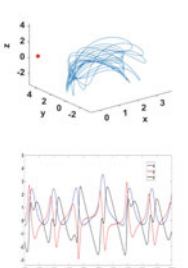
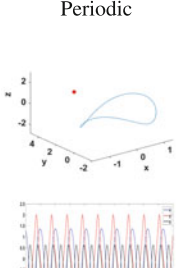
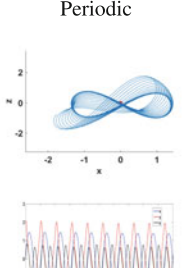
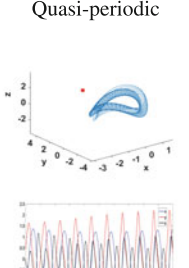
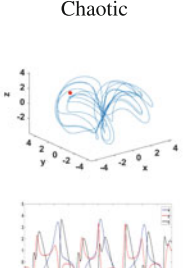
**Table 5** Response type of the dissipative system with hidden attractor at various values of fractional-order  $\alpha$  and parameter  $a$

	$\alpha = 0.96$	$\alpha = 0.98$	$\alpha = 1$
$a = 0.15$	<p>Periodic</p> 	<p>Periodic</p> 	<p>Chaotic</p> 
$a = 0.25$	<p>Periodic</p> 	<p>Periodic</p> 	<p>Chaotic</p> 
$a = 0.35$	<p>Divergence</p> 	<p>Periodic</p> 	<p>Chaotic</p> 
$a = 0.45$	<p>Divergence</p> 	<p>Periodic</p> 	<p>Chaotic</p> 

**Table 6** Response type of the dissipative system with self-excited attractor at various values of fractional-order  $\alpha$  and parameters  $a$  and  $b$

	$\alpha = 0.95$	$\alpha = 0.97$	$\alpha = 0.98$	$\alpha = 0.99$	$\alpha = 1$
$a = 0.6$ $b = 0.58$	Periodic 	Periodic 	Periodic 	Chaotic 	Chaotic 
$a = 1.2$ $b = 1.2$	Periodic 	Periodic 	Periodic 	Periodic 	Divergence 

**Table 7** Conservative system responses versus fractional-order  $\alpha$  and parameter  $a$

	$\alpha = 0.95$	$\alpha = 0.97$	$\alpha = 0.99$	$\alpha = 1$
$a = 1$	Periodic 	Periodic 	Chaotic 	Chaotic 
$a = 1.5$	Periodic 	Periodic 	Quasi-periodic 	Chaotic 

sections, transient regions of the time series and attractors are shown to illustrate that synchronization takes place early at the beginning of simulation time.

The dissipative system with hidden attractor exhibits a narrow range of fractional-orders that yield chaotic behavior and may exhibit divergent responses. Consequently, it is utilized in Sects. 6 and 7 as a slave system to control its response. For the dissipative system with self-excited attractor, the parameter  $c$  is just a scaling parameter [65], so the effect of  $a$ ,  $b$  as well as  $\alpha$  is considered.

## 5 Control and Switching Synchronization

In this section, a control and switching technique for synchronizing the response of any chaotic system to follow another pattern is presented. This can be achieved through two switches that control the role of each system whether it acts as a master or a slave. Figure 1 shows the general block diagram that describes the proposed technique for two chaotic systems. Conventional synchronization is defined as changing the response of the slave system to synchronize with the master chaotic system and exactly follow its pattern. This purpose is achieved using active control functions which affect only the slave response without any loading on the master system [7, 43].

The switching synchronization technique is applied to the Lü system and the Newton-Leipnik system. Hence, their equations with the switches and control functions effect being considered are given by:

$$D^\alpha x_1 = a_1(y_1 - x_1) - S_1 u_x, \quad (9a)$$

$$D^\beta y_1 = b_1 y_1 - x_1 z_1 - S_1 u_y, \quad (9b)$$

$$D^\gamma z_1 = x_1 y_1 - c_1 z_1 - S_1 u_z, \quad (9c)$$

and

$$D^\alpha x_2 = -a_2 x_2 + y_2 + 10y_2 z_2 + S_2 u_x, \quad (10a)$$

$$D^\beta y_2 = -x_2 - 0.4y_2 + 5x_2 z_2 + S_2 u_y, \quad (10b)$$

$$D^\gamma z_2 = b_2 z_2 - 5x_2 y_2 + S_2 u_z, \quad (10c)$$

where  $S_1$  and  $S_2$  are on-off parameters (digital bit), which either have the values “1” or “0” according to the required dependence between both systems as shown in Fig. 1. The unknown terms  $(u_x, u_y, u_z)$  in (9) and (10) are active control functions to be determined, and the error functions can be defined as:

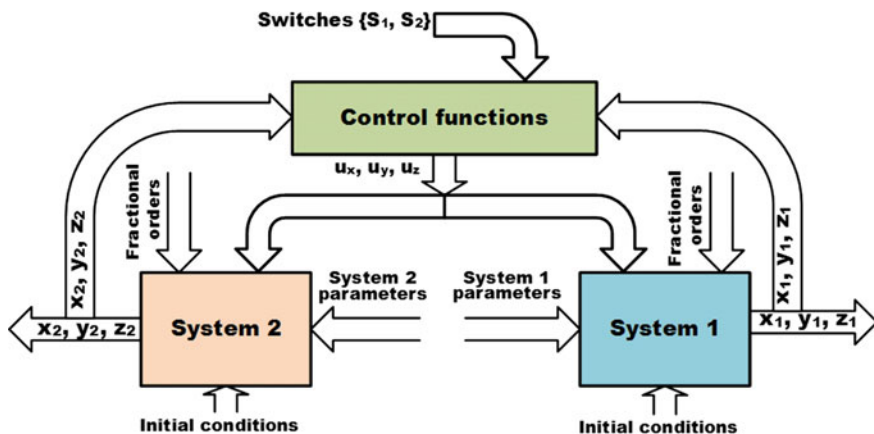


Fig. 1 Block diagram of the switched synchronization scheme between two different fractional-order chaotic systems

$$e_x = x_2 - x_1, e_y = y_2 - y_1, e_z = z_2 - z_1. \tag{11}$$

Equation (11) together with (9) and (10) yield the error system

$$D^\alpha e_x = -a_2(e_x + x_1) + (1 + 10(e_z + z_1))(e_y + y_1) - a_1(y_1 - x_1) + (S_1 + S_2)u_x, \tag{12a}$$

$$D^\beta e_y = -(e_x + x_1) - 0.4(e_y + y_1) + 5(e_x + x_1)(e_z + z_1) - b_1y_1 + x_1z_1 + (S_1 + S_2)u_y, \tag{12b}$$

$$D^\gamma e_z = b_2(e_z + z_1) - 5(e_x + x_1)(e_y + y_1) - x_1y_1 + c_1z_1 + (S_1 + S_2)u_z. \tag{12c}$$

The active control functions  $(u_x, u_y, u_z)$  are defined as follows

$$(S_1 + S_2)u_x = V_x(e_x) - (1 + 10(e_z + z_1))(e_y + y_1) + a_1(y_1 - x_1) + a_2x_1, \tag{13a}$$

$$(S_1 + S_2)u_y = V_y(e_y) + e_x + x_1 + (0.4 + b_1)y_1 - 5(e_x + x_1)(e_z + z_1) - x_1z_1, \tag{13b}$$

$$(S_1 + S_2)u_z = V_z(e_z) - (b_2 + c_1)z_1 + 5(e_x + x_1)(e_y + y_1) + x_1y_1. \tag{13c}$$

The terms  $V_x, V_y$  and  $V_z$  are linear functions of the error terms  $e_x, e_y$  and  $e_z$ . With the choice of  $u_x, u_y$  and  $u_z$  given by (13) the error system between the two chaotic systems (12) becomes

$$D^\alpha e_x = -a_2e_x + V_x(e_x), D^\beta e_y = -0.4e_y + V_y(e_y), D^\gamma e_z = b_2e_z + V_z(e_z). \tag{14}$$

There is no need to solve (14) if the solution converges to zero. Therefore, the control terms  $V_x$ ,  $V_y$  and  $V_z$  can be chosen such that the system (15) becomes stable with zero steady state.

$$\begin{pmatrix} V_x(e_x) \\ V_y(e_y) \\ V_z(e_z) \end{pmatrix} = A \begin{pmatrix} e_x \\ e_y \\ e_z \end{pmatrix}, \tag{15}$$

where  $A$  is a  $3 \times 3$  real matrix chosen so that all eigenvalues  $\lambda_i$  of the system (15) satisfy the following condition:

$$|\arg(\lambda_i)| > \frac{\alpha\pi}{2}. \tag{16}$$

Hence, the matrix  $A$  is chosen as follows

$$A = \begin{pmatrix} a_2 - k_x & 0 & 0 \\ 0 & 0.4 - k_y & 0 \\ 0 & 0 & -b_2 - k_z \end{pmatrix}. \tag{17}$$

Then the eigenvalues of the linear system (15) satisfy the necessary and sufficient condition (16) for all fractional-orders  $\alpha < 2$  [53]. In this specific case,  $k_x = k_y = k_z = 100$  is chosen to overcome the large difference between ranges of  $x$ ,  $y$  and  $z$  between the two chosen systems.

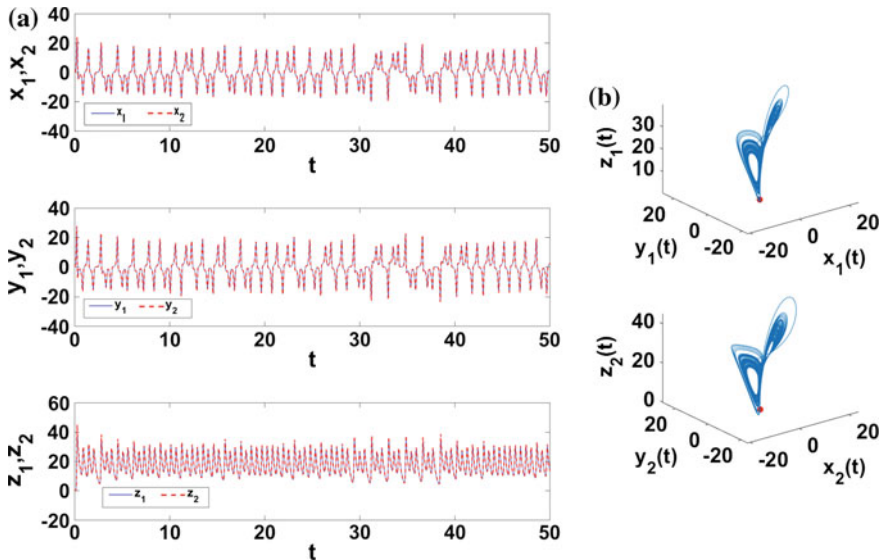


**Fig. 2** Static switching setting Lü as a master and Newton-Leipnik as a slave **a** Time series, **b** Attractor diagrams

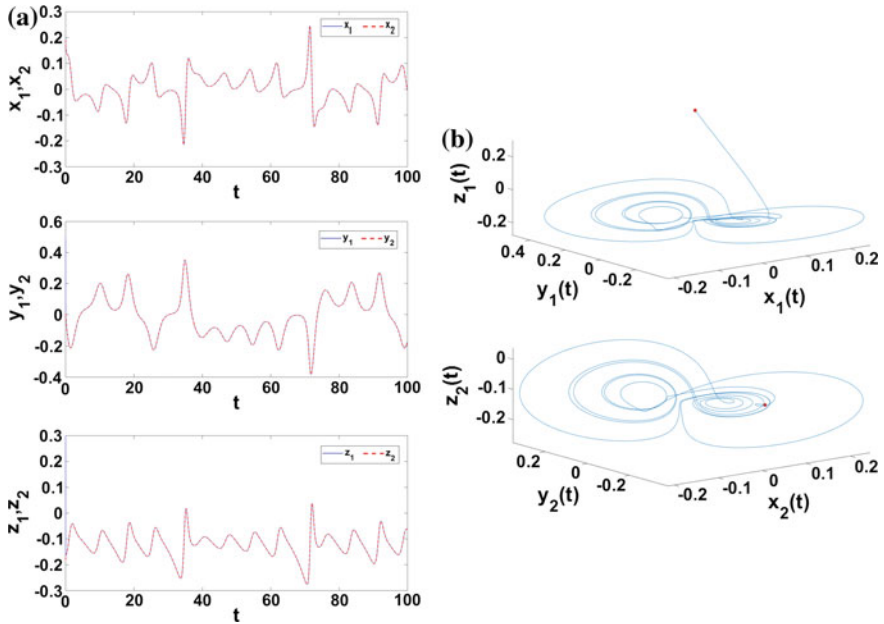


**Fig. 3** Static switching setting Newton-Leipnik as a master and Lü as a slave **a** Time series, **b** Attractor diagrams

Simulation results validate the previous analysis as shown in Fig. 2. Time series and attractor diagrams are shown for the case  $(S_1, S_2) = (0, 1)$  at  $(\alpha, \beta, \gamma) = (0.95, 0.96, 0.97)$ . Lü system works normally and the Newton-Leipnik system adapts its response to follow the Lü system. Time series of Lü are represented by the solid lines while the dotted lines correspond to those of Newton-Leipnik. Similarly, Fig. 3 shows time series and attractor diagrams in the reverse case when  $(S_1, S_2) = (1, 0)$ . Dynamic or mixed synchronization could also be achieved in which the switches become functions of time. In this case, the role of each system is not fixed throughout the simulation time, i.e., both systems can exchange their roles at any time instant.

## 6 Synchronization of Two Fractional-Order Chaotic Systems

### 6.1 Generalized Synchronization

Generalized synchronization aims at changing the response of the slave system to follow a given relation with the master system. Based on the active control method for synchronization and anti-synchronization [21] and the generalized synchroniza-

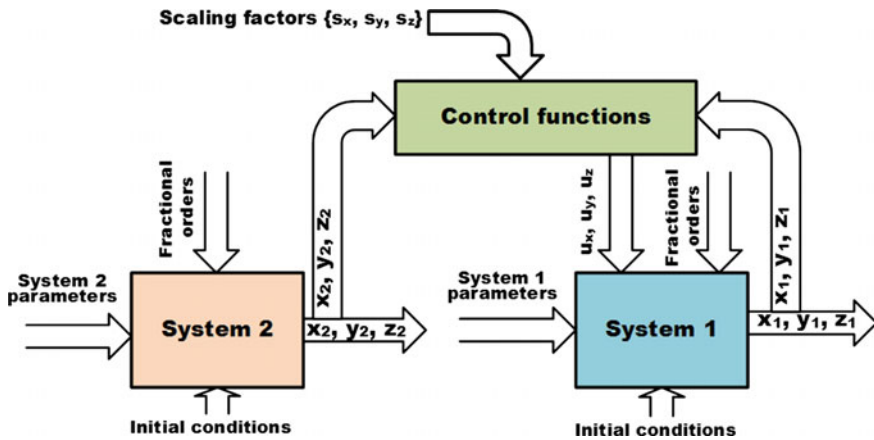


**Fig. 4** Block diagram of the generalized synchronization scheme between two different fractional-order chaotic systems

tion that has been applied to identical systems [43], a more general synchronization scheme is adapted as shown in Fig. 4 such that it becomes suitable for different systems too. For 3D phase space systems, the error vector between the generated responses of the two synchronized systems is given by

$$e = \begin{pmatrix} e_x \\ e_y \\ e_z \end{pmatrix} = \begin{pmatrix} x_m + s_x x_s \\ y_m + s_y y_s \\ z_m + s_z z_s \end{pmatrix}, \tag{18}$$

where  $(x_m, y_m, z_m)$  and  $(x_s, y_s, z_s)$  are the responses of the master and slave systems, respectively. Hence,

$$x_s(t) = -\frac{x_m(t)}{s_x(t)}, \quad y_s(t) = -\frac{y_m(t)}{s_y(t)}, \quad z_s(t) = -\frac{z_m(t)}{s_z(t)}. \tag{19}$$

This generalized synchronization permits various special cases to appear at different values of the scaling factors. The cases listed below are used in this section to validate the proposed generalized synchronization technique.

### 6.1.1 Case 1: Scaled Synchronization and Anti-synchronization

In this case, each  $s_i, i \in \{x, y, z\}$ , is a constant value which is time-independent. All responses ( $x, y$  and  $z$  for 3-D) could be scaled with the same factor or each with a different factor. For  $s_i$  negative, the slave response is in phase (synchronized) with the master response, while for positive values of  $s_i$  they have an opposite phase (anti-



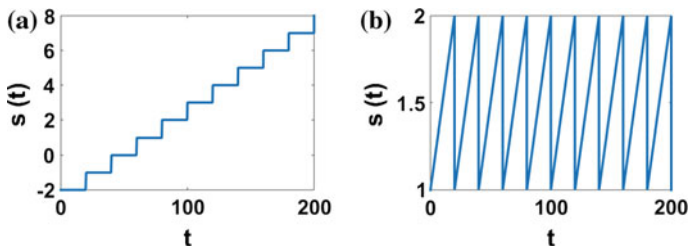


Fig. 5 Examples on scaling factors **a**  $s(t) = -2 + \text{int}(t/20)$  and **b**  $s(t) = 1 + (\text{mod}(t/20))/20$

synchronized). Moreover, when  $|s_i| < 1$ , the slave response has a higher amplitude than the master response, whereas it has a lower amplitude when  $|s_i| > 1$  according to (19).

### 6.1.2 Case 2: Scaling Factors $s_i(t)$ Are Functions of Time

Multiple cases in which  $s_i$  is a function of time could be described. For example,  $s_i(t) = c + \text{int}(t/m)$ , where  $c, m$  are constants and  $\text{int}(\cdot)$  returns the quotient of integer division. This is a stair-case function which performs scaling in a variable manner as time advances. The type of synchronization (anti-synchronization) and/or its scale change every  $m$  time units as the example shown in Fig. 5a. Another example is  $s_i(t) = c + (\text{mod}(t/m))/m$ , where  $c, m$  are constants and  $\text{mod}(\cdot)$  returns the remainder of integer division. This is a periodic ramp function which is time-dependent too. The value of the scaling factor increases within every interval of  $m$  time units and resets at the end of each interval as the example shown in Fig. 5b.

## 6.2 Simulation Results for Two Fractional-Order Systems

First, we consider generalized synchronization of two identical systems in which only parameters and/or initial conditions differ. For this purpose, fractional-order Chua's circuit is used which is a 4-D system. The slave (response) and master (drive) systems are described, respectively, by the following equations. However, the initial condition of the drive system is different from that of the response system.

$$\begin{aligned} D^\alpha x_1 &= a_1(y_1 - f(w_1)x_1) + u_x, & D^\beta y_1 &= z_1 - x_1 + u_y, \\ D^\gamma z_1 &= -b_1y_1 + c_1z_1 + u_z, & Dw_1 &= x_1 + u_w. \end{aligned} \quad (20)$$

$$\begin{aligned} D^\alpha x_2 &= a_2(y_2 - f(w_2)x_2), \quad D^\beta y_2 = z_2 - x_2, \\ D^\gamma z_2 &= -b_2y_2 + c_2z_2, \quad Dw_2 = x_2. \end{aligned} \tag{21}$$

Extending Eq. (18) to 4-D, substituting in it and calculating the fractional derivatives of the error functions, the set of Eq. (22) is obtained.

$$D^\alpha e_x = a_2(y_2 - f(w_2)x_2) + s_x(a_1(y_1 - f(w_1)x_1) + u_x), \tag{22a}$$

$$D^\alpha e_y = z_2 - x_2 + s_y(z_1 - x_1 + u_y), \tag{22b}$$

$$D^\alpha e_z = -b_2y_2 + c_2z_2 + s_z(-b_1y_1 + c_1z_1 + u_z), \tag{22c}$$

$$D^\alpha e_w = x_2 + s_w(x_1 + u_w). \tag{22d}$$

For the purpose of synchronization, all terms except those which are function of the corresponding error term should be canceled. For example, in the equation of  $D^\alpha e_x$  only  $e_x$  should appear. Hence, the vector of control functions  $u$  is given by:

$$u_x = \frac{1}{s_x} (-a_2(y_2 - f(w_2)x_2) - s_x(-a_1(y_1 - f(w_1)x_1)) - k_x e_x), \tag{23a}$$

$$u_y = \frac{1}{s_y} (-z_2 + x_2 - s_y(z_1 - x_1) - k_y e_y), \tag{23b}$$

$$u_z = \frac{1}{s_z} (b_2y_2 - c_2z_2 - s_z(-b_1y_1 + c_1z_1) - k_z e_z), \tag{23c}$$

$$u_w = \frac{1}{s_w} (-x_2 - s_w x_1 - k_w e_w), \tag{23d}$$

which result in decaying error functions as the values of  $k_x, k_y, k_z$  and  $k_w$  are positive. The procedure is simple for this case, however, a more detailed analysis for the general case is provided in Sect. 7.

Figure 6 shows samples of successfully achieved generalized synchronization between the slave and master system at  $(\alpha, \beta, \gamma) = (0.93, 0.95, 0.97)$  for different parameter values  $(a_1, b_1, c_1) = (4.5, 0.9, 0.6)$  and  $(a_2, b_2, c_2) = (4, 1, 0.65)$  and starting at different initial conditions  $(x_{10}, y_{10}, z_{10}, w_{10}) = (0.02, 0.03, 0.02, 0.06)$  and  $(x_{20}, y_{20}, z_{20}, w_{20}) = (0.01, 0.02, 0.01, 0.05)$ .

Figure 6a shows static synchronization with  $s_x = -3$  where the  $x$ -time series of the slave synchronizes with that of the master system at a scaling factor of  $(1/3)$ . Figure 6b shows static synchronization with  $s_y = 0.25$  where the  $y$ -time series of

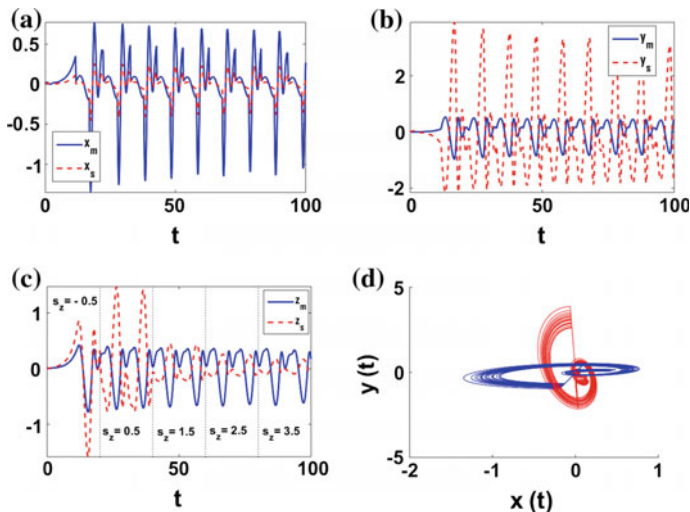


**Fig. 6** Generalized synchronization of Chua’s circuit at **a**  $s_x = -3$ , **b**  $s_y = 0.25$ , **c**  $s_z = -0.5 + int(t/20)$  and **d** Attractor diagrams of the slave system (in red) different from the original attractor (in blue)

the slave is anti-synchronized with that of the master system at a scaling factor of 4. Figure 6c shows dynamic synchronization at  $s_z(t) = -0.5 + int(t/20)$  where the scaling factor starts with a value equals  $-0.5$  and increases by 1 every 20 time units. Figure 6d shows the resulting attractor diagram with new shape after applying these scaling functions.

Further simulation results are also presented to illustrate the generalized synchronization of two different fractional-order systems whether they generate periodic or chaotic responses. The following equations represent a dissipative hidden attractor [25] as the slave system (system 1) as well as a dissipative self-excited attractor [65] (system 2) and a conservative system [25] (system 3) as the master systems alternatively.

$$D^\alpha x_1 = -y_1 + u_x, \quad D^\beta y_1 = x_1 + z_1 + u_y, \quad D^\gamma z_1 = 2y_1^2 + x_1z_1 - a_1 + u_z. \tag{24}$$

$$D^\alpha x_2 = y_2, \quad D^\beta y_2 = z_2, \quad D^\gamma z_2 = -y_2 - a_2z_2 + b_2 \left( \frac{x_2^2}{c_2} - c_2 \right). \tag{25}$$

$$D^\alpha x_3 = y_3, \quad D^\beta y_3 = -x_3 - z_3y_3, \quad D^\gamma z_3 = y_3^2 - a_3. \tag{26}$$

The methodology of obtaining the control signals using active nonlinear control method is performed similar to the previous section and as discussed in [44].

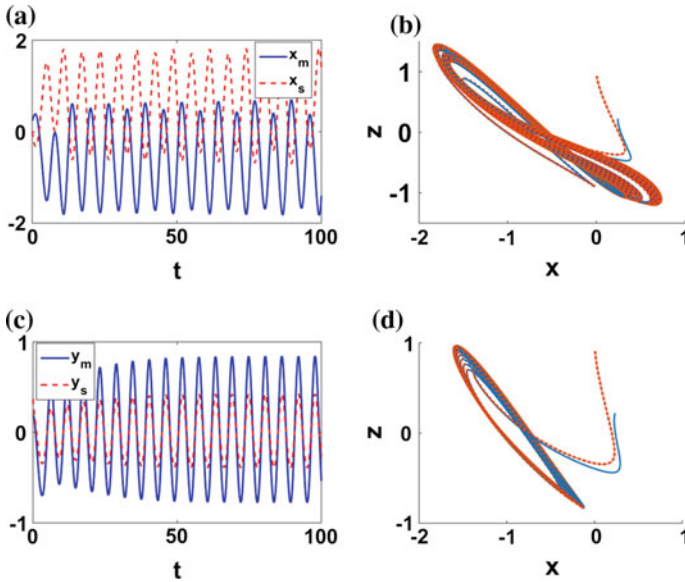
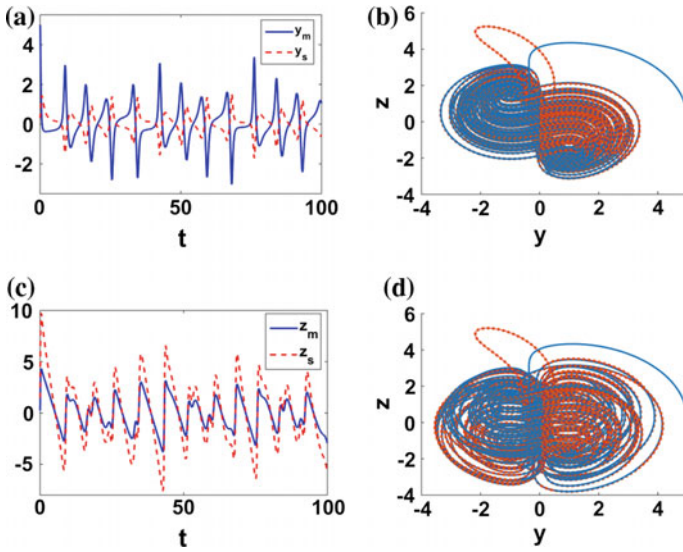


**Fig. 7** Static synchronization (Case 1) with system 2 as master and system 1 as slave at **a**  $\{\alpha, \beta, \gamma\} = \{0.97, 1, 0.95\}$  and  $s_x = 1$ , **b**  $s_x = s_y = s_z = -1$ , **c**  $\{\alpha, \beta, \gamma\} = \{0.93, 0.93, 0.93\}$  and  $s_y = -2$ , and **d**  $s_x = s_y = s_z = -1$

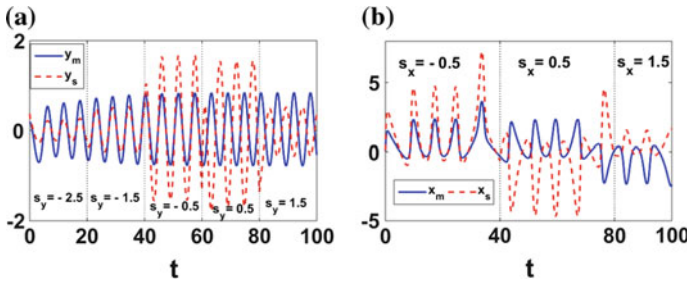
Consider the synchronization of the slave system with system 2 as the master system. The plots in Fig. 7 match the expected behavior where at  $s_x = 1$ , the slave response is the exact anti-synchronization of the master response, and at  $s_y = -2$  it is the halved-synchronization. The master and slave attractor diagrams are shown to be co-incident in the case of full-synchronization  $s_x = s_y = s_z = -1$ . It is worth mentioning that the system exhibits different attractors when varying the values of fractional-orders as illustrated by the two  $y$ - $z$  projections plotted at  $\{\alpha, \beta, \gamma\} = \{0.97, 1, 0.95\}$  and  $\{\alpha, \beta, \gamma\} = \{0.93, 0.93, 0.93\}$ .

Figure 8 shows the synchronization of the slave system with system 3 as the master system. The integer-order case, or autonomous system of three first order ordinary differential equations, is shown to follow the same expected behavior as a special case of generalized fractional-order.

Figure 9 shows dynamic synchronization at  $s_y(t) = -2.5 + int(t/20)$  where the scaling factor starts with a value of  $-2.5$  and increases by 1 every 20 time units. It also shows dynamic synchronization at  $s_x = -0.5 + int(t/40)$  where the scaling factor starts with a value of  $-0.5$  and increases by 1 every 40 time units.



**Fig. 8** Static synchronization (Case 1) with system 3 as master and system 1 as slave at **a**  $\{\alpha, \beta, \gamma\} = \{1, 1, 1\}$  and  $s_y = 2$ , **b**  $s_x = s_y = s_z = -1$ , **c**  $\{\alpha, \beta, \gamma\} = \{0.97, 1, 0.99\}$  and  $s_z = -0.5$ , and **d**  $s_x = s_y = s_z = -1$



**Fig. 9** Dynamic synchronization (Case 2) with system 2 as master and system 1 as slave at **a**  $\{\alpha, \beta, \gamma\} = \{0.93, 0.93, 0.93\}$  and  $s_y = -2.5 + int(t/20)$  and **b**  $\{\alpha, \beta, \gamma\} = \{0.97, 1, 0.99\}$  and  $s_x = -0.5 + int(t/40)$

## 7 Synchronization of a Fractional-Order Chaotic System and a Linear Combination of Two Other Systems

In this section, a novel fractional-order chaotic system is formed as a linear combination of two fractional-order systems and another system is synchronized with this linear combination. This linear combination represents another means of controlling the system response and forcing it to yield chaos. The block diagram of the generalized synchronization scheme is shown in Fig. 10 where the linear combination of systems 2 and 3 is the master and system 1 is the slave.

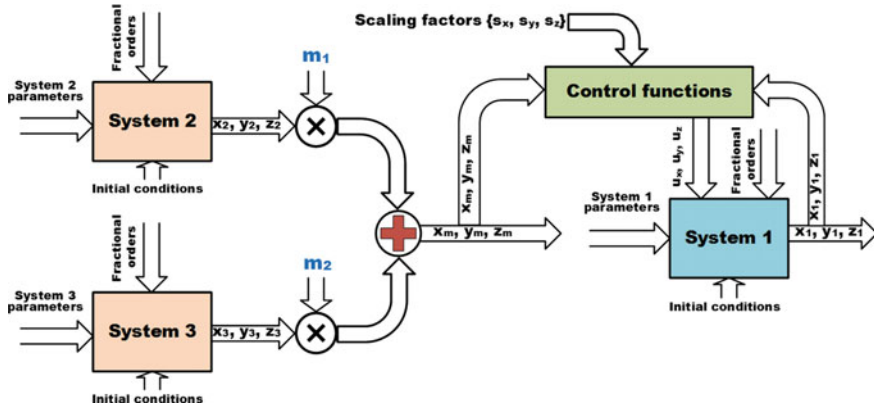


Fig. 10 Block diagram of generally synchronizing a fractional-order chaotic system with a linear combination of two systems

Table 8 shows the attractor diagrams of different linear combinations of systems 2 and 3 at various values of fractional-orders where the post-transient part is colored in blue. Several examples show that the linear combination can yield more chaotic responses or sequences with long periods in fractional-order in comparison with the single systems shown in Tables 6 and 7. These cases can be proven to exhibit chaotic behavior through well-known techniques such as maximum Lyapunov exponent calculation.

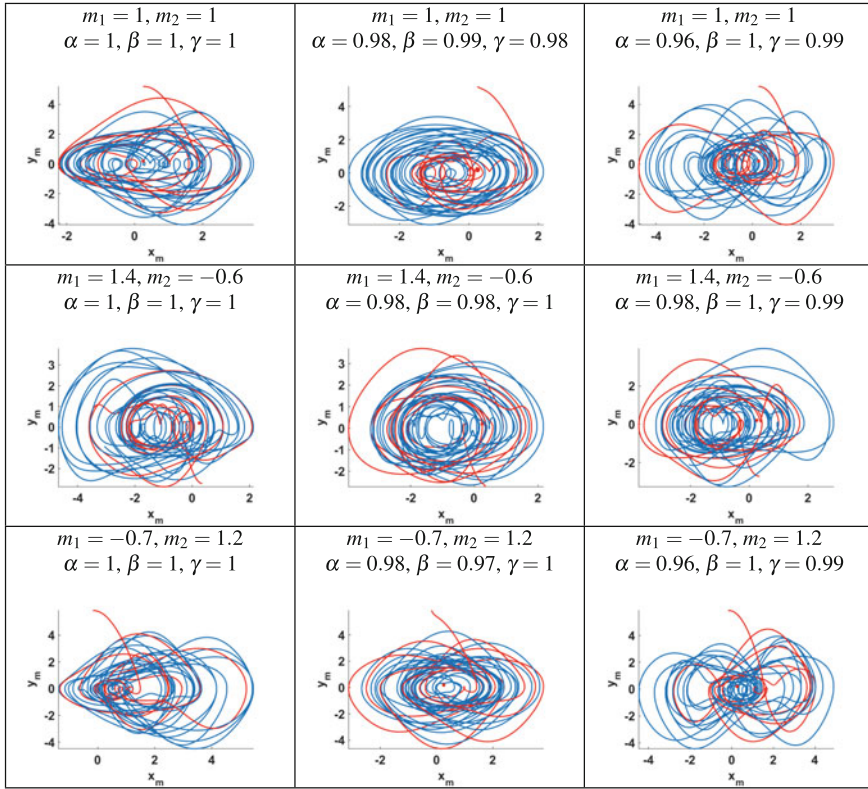
The procedure in [44] is applied but with an added capability of generalized synchronization with the cases explained in Sect. 6. As previously mentioned, all state variables, scaling factors and control functions are in general functions of time. The combined responses of the two systems shown in Fig. 10 can be written as:

$$x_m = m_1 x_2 + m_2 x_3, \tag{27a}$$

$$y_m = m_1 y_2 + m_2 y_3, \tag{27b}$$

$$z_m = m_1 z_2 + m_2 z_3, \tag{27c}$$

substituting in (18) and calculating the fractional derivatives, the set of equations (28) is obtained. For the purpose of synchronization, all terms except those which are function of the corresponding error term should be canceled. For example, in the equation of  $D^\alpha e_x$  only  $e_x$  should appear. Hence, the vector of control functions  $u$  is given by (29).

**Table 8** Attractor diagrams of different linear combinations of systems 2 and 3 at various values of fractional-orders

$$\begin{aligned}
 D^\alpha e_x &= D^\alpha (x_m + s_x x_s) = D^\alpha (m_1 x_2 + m_2 x_3 + s_x x_1) = m_1 y_2 + m_2 y_3 - s_x y_1 + s_x u_x \\
 &= m_1 y_2 + m_2 y_3 - s_x \left( \frac{e_y - y_m}{s_y} \right) + s_x u_x, \quad (28a)
 \end{aligned}$$

$$\begin{aligned}
 D^\beta e_y &= D^\beta (y_m + s_y y_s) = D^\beta (m_1 y_2 + m_2 y_3 + s_y y_1) \\
 &= m_1 z_2 - m_2 x_3 - m_2 z_3 y_3 + s_y x_1 + s_y z_1 + s_y u_y \\
 &= m_1 z_2 - m_2 x_3 - m_2 z_3 y_3 + s_y \left( \frac{e_x - x_m}{s_x} \right) + s_y \left( \frac{e_z - z_m}{s_z} \right) + s_y u_y, \quad (28b)
 \end{aligned}$$

$$\begin{aligned}
 D^\gamma e_z &= D^\gamma (z_m + s_z z_s) \\
 &= -m_1 y_2 - m_1 a_2 z_2 + m_1 b_2 \left( \frac{x_2^2}{c_2} - c_2 \right) + m_2 y_3^2 - m_2 a_3 \\
 &\quad + 2s_z y_1^2 + s_z x_1 z_1 - s_z a_1 + s_z u_z \\
 &= -m_1 \left( y_2 + a_2 z_2 - b_2 \left( \frac{x_2^2}{c_2} - c_2 \right) \right) + m_2 (y_3^2 - a_3) \\
 &\quad + s_z \left( 2 \left( \frac{e_y - y_m}{s_y} \right)^2 + \left( \frac{e_x - x_m}{s_x} \right) \left( \frac{e_z - z_m}{s_z} \right) - a_1 + u_z \right). \tag{28c}
 \end{aligned}$$

Therefore, the control functions can be obtained by using (15) as follows:

$$u_x = V_x(e_x) - \frac{m_1}{s_x} y_2 - \frac{m_2}{s_x} y_3 - \frac{1}{s_y} y_m + \frac{1}{s_y} e_y = V_x(e_x) - \frac{1}{s_x} y_m - \frac{1}{s_y} y_m + \frac{1}{s_y} e_y, \tag{29a}$$

$$u_y = V_y(e_y) - \frac{m_1}{s_y} z_2 + \frac{m_2}{s_y} x_3 + \frac{m_2}{s_y} z_3 y_3 + \frac{1}{s_x} x_m + \frac{1}{s_z} z_m - \frac{1}{s_x} e_x - \frac{1}{s_z} e_z, \tag{29b}$$

$$\begin{aligned}
 u_z &= V_z(e_z) + \frac{m_1}{s_z} y_2 + \frac{m_1}{s_z} a_2 z_2 - \frac{m_1}{s_z} b_2 \left( \frac{x_2^2}{c_2} - c_2 \right) - \frac{m_2}{s_z} y_3^2 + \frac{m_2}{s_z} a_3 \\
 &\quad - 2 \left( \frac{e_y - y_m}{s_y} \right)^2 - \left( \frac{e_x - x_m}{s_x} \right) \left( \frac{-z_m}{s_z} \right) + a_1. \tag{29c}
 \end{aligned}$$

Recalling that  $(e_x - x_m)/s_x = x_1$  from (18), the following equations for fractional derivatives of error are, thus, obtained:

$$D^\alpha e_x = s_x V_x(e_x), \tag{30a}$$

$$D^\beta e_y = s_y V_y(e_y), \tag{30b}$$

$$D^\gamma e_z = s_z V_z(e_z) + x_1 e_z. \tag{30c}$$

Based on the nonlinear control theory and Lyapunov stability theory [53], these derivatives should be decaying functions of the error. The terms  $V_x(e_x)$ ,  $V_y(e_y)$ , and  $V_z(e_z)$  form a system of linear equations in the errors  $e_x$ ,  $e_y$ , and  $e_z$ . They should be chosen carefully to form a stable system with zero steady state [44]. Consequently, they should force negative eigen values for the synchronization system:



$$\begin{pmatrix} V_x(e_x) \\ V_y(e_y) \\ V_z(e_z) \end{pmatrix} = \begin{pmatrix} -\frac{k_x}{s_x} & 0 & 0 \\ 0 & -\frac{k_y}{s_y} & 0 \\ 0 & 0 & -\left(\frac{k_z+x_1}{s_z}\right) \end{pmatrix} \begin{pmatrix} e_x \\ e_y \\ e_z \end{pmatrix}. \tag{31}$$

Here, the coefficients  $k_x, k_y, k_z$  are simply chosen as ones. It could be proved, similar to [43, 44], that the designed controller achieves the general required synchronization function.

Simulation results are presented, which validate the synchronization of a chaotic system with a linear combination of two other systems. The plots shown in Figs. 11, 12 and 13 match the explanation of different cases of generalized synchronization explained in Sect. 6 with the same parameters and initial values given in Table 1. Various generalized static and dynamic synchronization cases for different values of the linear combination’s coefficients  $m_1$  and  $m_2$  are demonstrated.

The case  $m_1 = m_2 = 1$  represents synchronizing the slave system with the sum of the two other systems. In addition, the response of the slave system follows the selected synchronization case among the cases illustrated in Sect. 6 and according to (19). For example, when  $s_x = 0.5$ ,  $x$ -time series of the slave system is the doubled anti-synchronization of that of the linear combination (master system). When  $s_z(t) = 1 + (\text{mod}(t/50))/50$ , the  $z$ -time series of the slave starts as the exact anti-synchronized version of that corresponding to the master. Then, the scaling factor

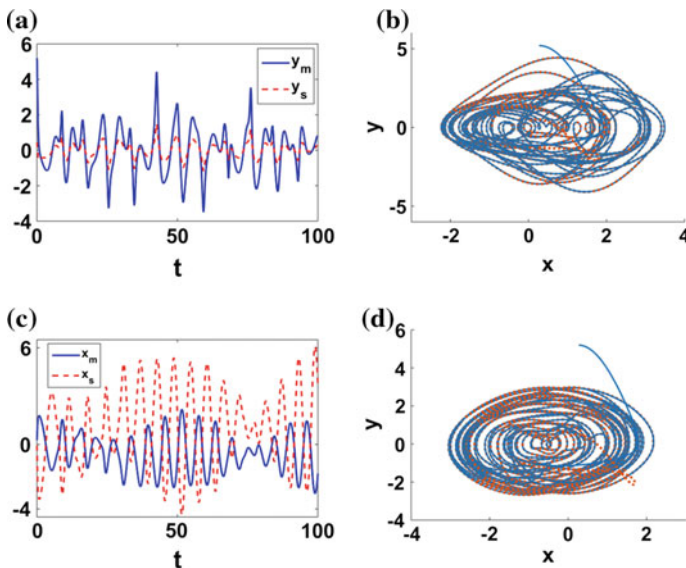


**Fig. 11** Static synchronization (Case 1) of system 1 with a linear combination of systems 2 and 3 at  $m_1 = m_2 = 1$  and **a**  $\{\alpha, \beta, \gamma\} = \{1, 1, 1\}$  and  $s_y = -3$ , **b**  $s_x = s_y = s_z = -1$ , **c**  $\{\alpha, \beta, \gamma\} = \{0.97, 1, 0.95\}$  and  $s_x = 0.5$ , and **d**  $s_x = s_y = s_z = -1$

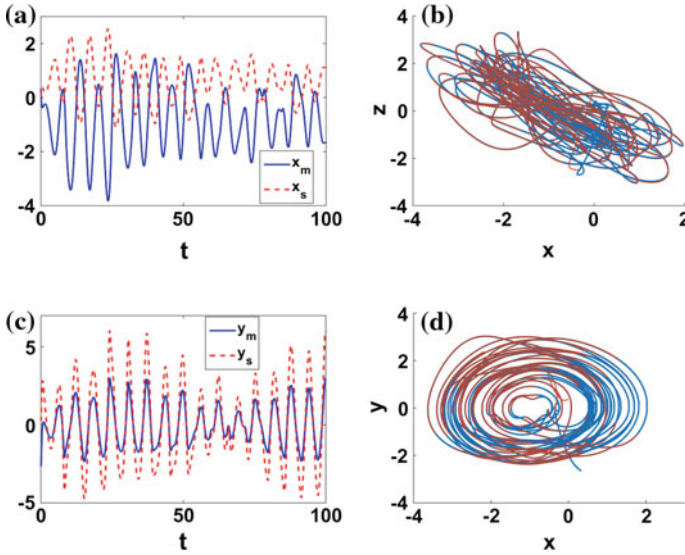


**Fig. 12** Static synchronization (Case 1) of system 1 with a linear combination of systems 2 and 3 at  $m_1 = 1.4$  and  $m_2 = -0.6$  and **a**  $\{\alpha, \beta, \gamma\} = \{0.97, 0.99, 0.99\}$  and  $s_x = 1.5$ , **b**  $s_x = s_y = s_z = -1$ , **c**  $\{\alpha, \beta, \gamma\} = \{0.98, 0.98, 0.98\}$  and  $s_y = -0.5$ , and **d**  $s_x = s_y = s_z = -1$

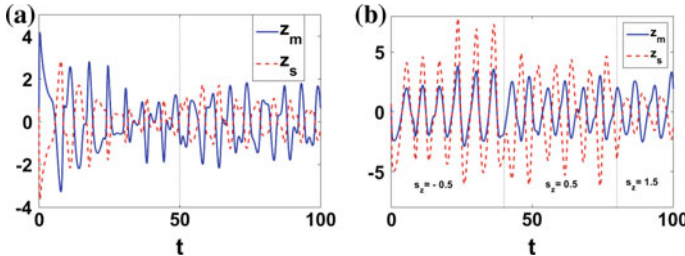


**Fig. 13** Dynamic synchronization (Case 2) **a**  $m_1 = m_2 = 1$ ,  $\{\alpha, \beta, \gamma\} = \{0.97, 1, 0.95\}$  and  $s_z = 1 + (\text{mod}(t/50))/50$  and **b**  $m_1 = 2$  and  $m_2 = -0.5$ ,  $\{\alpha, \beta, \gamma\} = \{0.98, 0.98, 0.98\}$  and  $s_z = -0.5 + \text{int}(t/40)$

increases gradually such that the amplitude of the slave system decreases till  $t = 50$ . At  $t = 50$ , the system returns to exact anti-synchronization followed by the gradual decrease in the amplitude of the slave. Synchronization at other values of  $m_1$  and  $m_2$  could be described similarly, e.g.,  $m_1 = 1.4$  and  $m_2 = -0.6$  shown in Fig. 12. The resulting attractor diagram is usually similar to that of the system which has a higher value for the coefficient, or weight.

The time series at values of fractional-orders around those in Figs. 11, 12 and 13 show that the response of the linear combination is chaotic, i.e., the values do not repeat. Setting  $m_1 = 1$  and  $m_2 = 0$ , or alternatively  $m_1 = 0$  and  $m_2 = 1$ , yields the same results as those in Sect. 6. Other values for the coefficients are possible and yield consistent results too.

## 8 Conclusions

Six chaotic systems were selected and utilized in their fractional-order form to analyze and validate three proposed block diagrams of synchronization systems. Discretized solutions to the systems were obtained using the Grünwald-Letnikov method of approximation and the nonstandard finite difference method for discretization. Synchronization techniques were based on active nonlinear control and Lyapunov stability. The nonlinear controller is designed to ensure the stability and convergence of the proposed synchronization scheme.

The first block diagram presents a switching synchronization scheme between two different chaotic systems or one chaotic system with different parameters using the active control method. By using the proposed technique, it is possible to perform static synchronization (switching control independent of time), mono-dynamic synchronization (one of the control switches depends on time) or bi-dynamic synchronization (the two switches are time dependent). The concepts introduced in this block diagram have been verified by using the fractional-order version of two different known chaotic systems, which are the Lü and the Newton-Leipnik chaotic systems. Moreover, the switching parameters can be a function of time to introduce a new concept of static and dynamic switching of synchronizations, which makes the system more flexible as shown from the results.

The second block diagram presents a generalized synchronization scheme that has been validated to work for different chaotic systems as well as identical systems. This generalized synchronization permits both static and dynamic synchronization or anti-synchronization with various scaling factors. Hence, conventional synchronization is considered a very narrow subset from the proposed technique where the scale between the output response and the input response can be controlled via control functions and this scale may be either constant (positive, negative) or time dependent. Many examples including synchronization and anti-synchronization, between identical or different systems with the same or different system parameters and initial conditions, are discussed. The scaling functions are chosen to be positive/negative and constant/dynamic, which covers all possible cases.

The proposed technique utilizing dynamic scaling functions can be useful in amplitude modulation applications in which the amplitude of the output signal should be a function of the input signal. The scaling factors in this case play the role of information signal, which is modulated by the chaotic dynamics of the system to give the modulated signal. Demodulation can be done similarly by reversing the operation.

Finally, a new chaotic system, constructed as a linear combination of two different systems, was introduced with two extra parameters that correspond to more degrees of freedom and response controlling capability. The generalized synchronization method was shown to successfully synchronize a third system with the system formed by the linear combination through both mathematical analysis and simulation results. All cases of the generalized synchronization scheme were validated in generalized fractional-order domain, with integer-order as a special case,

for different choices of the linear combination's coefficients and values of the scaling factors. Time series for various system responses and attractor diagrams were plotted to demonstrate different cases of generalized synchronization.

## References

1. Abd-El-Hafiz, S. K., Radwan, A. G., & AbdElHaleem, S. H. (2015). Encryption applications of a generalized chaotic map. *Applied Mathematics & Information Sciences*, 9(6), 1–19.
2. Abd-El-Hafiz, S. K., AbdElHaleem, S. H., & Radwan, A. G. (2016). Novel permutation measures for image encryption algorithms. *Optics and Lasers in Engineering*, 85, 72–83.
3. Agrawal, S., Srivastava, M., & Das, S. (2012). Synchronization of fractional order chaotic systems using active control method. *Chaos, Solitons & Fractals*, 45(6), 737–752.
4. Azar, A. T., & Vaidyanathan, S. (2015). *Chaos modeling and control systems design*. Springer.
5. Azar, A. T., & Vaidyanathan, S. (2016). *Advances in chaos theory and intelligent control* (Vol. 337). Springer.
6. Barakat, M. L., Mansingka, A. S., Radwan, A. G., & Salama, K. N. (2013). Generalized hardware post-processing technique for chaos-based pseudorandom number generators. *ETRI Journal*, 35(3), 448–458.
7. Bhalekar, S., & Daftardar-Gejji, V. (2010). Synchronization of different fractional order chaotic systems using active control. *Communications in Nonlinear Science and Numerical Simulation*, 15(11), 3536–3546.
8. Boulkroune, A., Bouzeriba, A., Bouden, T., & Azar, A. T. (2016a). Fuzzy adaptive synchronization of uncertain fractional-order chaotic systems. In *Advances in chaos theory and intelligent control* (pp. 681–697). Springer.
9. Boulkroune, A., Hamel, S., Azar, A. T., & Vaidyanathan, S. (2016b). Fuzzy control-based function synchronization of unknown chaotic systems with dead-zone input. In *Advances in chaos theory and intelligent control* (pp. 699–718). Springer.
10. Caponetto, R. (2010). *Fractional order systems: Modeling and control applications* (Vol. 72). World Scientific.
11. Chen, D., Zhang, R., Ma, X., & Liu, S. (2012). Chaotic synchronization and anti-synchronization for a novel class of multiple chaotic systems via a sliding mode control scheme. *Nonlinear Dynamics*, 69(1–2), 35–55.
12. Chen, D., Wu, C., Iu, H. H., & Ma, X. (2013). Circuit simulation for synchronization of a fractional-order and integer-order chaotic system. *Nonlinear Dynamics*, 73(3), 1671–1686.
13. Chen, S., & Lü, J. (2002). Synchronization of an uncertain unified chaotic system via adaptive control. *Chaos, Solitons & Fractals*, 14(4), 643–647.
14. Chien, T. I., & Liao, T. L. (2005). Design of secure digital communication systems using chaotic modulation, cryptography and chaotic synchronization. *Chaos, Solitons & Fractals*, 24(1), 241–255.
15. Faieghi, M. R., & Delavari, H. (2012). Chaos in fractional-order Genesio-Tesi system and its synchronization. *Communications in Nonlinear Science and Numerical Simulation*, 17(2), 731–741.
16. Frey, D. R. (1993). Chaotic digital encoding: An approach to secure communication. *IEEE Transactions on Circuits and Systems II: Analog and Digital Signal Processing*, 40(10), 660–666.
17. Gorenflo, R., & Mainardi, F. (1997). *Fractional calculus*. Springer.
18. Han, S. K., Kurrer, C., & Kuramoto, Y. (1995). Dephasing and bursting in coupled neural oscillators. *Physical Review Letters*, 75(17), 3190.
19. Henein, M. M. R., Sayed, W. S., Radwan, A. G., & Abd-El-Hafiez, S. K. (2016). Switched active control synchronization of three fractional order chaotic systems. In *13th International*

- Conference on Electrical Engineering/Electronics, Computer, Telecommunications and Information Technology.*
20. Hirsch, M. W., Smale, S., & Devaney, R. L. (2012). *Differential equations, dynamical systems, and an introduction to chaos*. Academic Press.
  21. Ho, M., Hung, Y., & Chou, C. (2002). Phase and anti-phase synchronization of two chaotic systems by using active control. *Physics Letters A*, 296(1), 43–48.
  22. Mc, Ho, & Hung, Y. C. (2002). Synchronization of two different systems by using generalized active control. *Physics Letters A*, 301(5), 424–428.
  23. Hosseinnia, S., Ghaderi, R., Mahmoudian, M., Momani, S., et al. (2010). Sliding mode synchronization of an uncertain fractional order chaotic system. *Computers & Mathematics with Applications*, 59(5), 1637–1643.
  24. Hussian, G., Alnaser, M., & Momani, S. (2008). Non-standard discretization of fractional differential equations. In: *Proceeding of 8th Seminar of Differential Equations and Dynamical Systems in, Isfahan, Iran*.
  25. Jafari, S., Sprott, J. C., & Golpayegani, S. M. R. H. (2013). Elementary quadratic chaotic flows with no equilibria. *Physics Letters A*, 377(9), 699–702.
  26. Kocarev, L., & Lian, S. (2011). *Chaos-based cryptography: Theory, algorithms and applications* (vol. 354). Springer.
  27. Lau, F., & Tse, C. K. (2003). *Chaos-based digital communication systems*. Springer.
  28. Li, C., & Yan, J. (2007). The synchronization of three fractional differential systems. *Chaos, Solitons & Fractals*, 32(2), 751–757.
  29. Liu, J., Ye, C., Zhang, S., & Song, W. (2000). Anti-phase synchronization in coupled map lattices. *Physics Letters A*, 274(1), 27–29.
  30. Magin, R. L. (2006). *Fractional calculus in bioengineering*. Begell House Redding.
  31. Mickens, R. E. (2000). *Applications of nonstandard finite difference schemes*. World Scientific.
  32. Mickens, R. E. (2005). *Advances in the applications of nonstandard finite difference schemes*. World Scientific.
  33. Moaddy, K., Radwan, A. G., Salama, K. N., Momani, S., & Hashim, I. (2012). The fractional-order modeling and synchronization of electrically coupled neuron systems. *Computers & Mathematics with Applications*, 64(10), 3329–3339.
  34. Odibat, Z. M., Corson, N., Aziz-Alaoui, M., & Bertelle, C. (2010). Synchronization of chaotic fractional-order systems via linear control. *International Journal of Bifurcation and Chaos*, 20(01), 81–97.
  35. Ouannas, A., Azar, A. T., & Abu-Saris, R. (2016a). A new type of hybrid synchronization between arbitrary hyperchaotic maps. *International Journal of Machine Learning and Cybernetics*, 1–8.
  36. Ouannas, A., Azar, A. T., & Vaidyanathan, S. (2016b). A robust method for new fractional hybrid chaos synchronization. *Mathematical Methods in the Applied Sciences*.
  37. Park, J., & Kwon, O. (2005). A novel criterion for delayed feedback control of time-delay chaotic systems. *Chaos, Solitons & Fractals*, 23(2), 495–501.
  38. Pecora, L. M., & Carroll, T. L. (1990). Synchronization in chaotic systems. *Physical Review Letters*, 64(8), 821.
  39. Petras, I. (2011). *Fractional-order nonlinear systems: Modeling, analysis and simulation*. Springer Science & Business Media.
  40. Radwan, A. (2012). Stability analysis of the fractional-order  $RL_{\beta}C_{\alpha}$  circuit. *Journal of Fractional Calculus and Applications*, 3(1), 1–15.
  41. Radwan, A., Soliman, A., & El-Sedeek, A. (2004). MOS realization of the modified Lorenz chaotic system. *Chaos, Solitons & Fractals*, 21(3), 553–561.
  42. Radwan, A., Soliman, A. M., & Elwakil, A. S. (2007). 1-D digitally-controlled multiscroll chaos generator. *International Journal of Bifurcation and Chaos*, 17(01), 227–242.
  43. Radwan, A., Moaddy, K., & Hashim, I. (2013). Amplitude modulation and synchronization of fractional-order memristor-based Chua's circuit. In *Abstract and applied analysis* (Vol. 2013). Hindawi Publishing Corporation.

44. Radwan, A., Moaddy, K., Salama, K. N., Momani, S., & Hashim, I. (2014a). Control and switching synchronization of fractional order chaotic systems using active control technique. *Journal of advanced research*, 5(1), 125–132.
45. Radwan, A. G. (2013a). On some generalized discrete logistic maps. *Journal of advanced research*, 4(2), 163–171.
46. Radwan, A. G. (2013b). Resonance and quality factor of the fractional circuit. *IEEE Journal on Emerging and Selected Topics in Circuits and Systems*, 3(3), 377–385.
47. Radwan, A. G., & Abd-El-Hafiz, S. K. (2013). Image encryption using generalized tent map. In *IEEE 20th International Conference on Electronics, Circuits, and Systems (ICECS)* (pp. 653–656). IEEE.
48. Radwan, A. G., & Abd-El-Hafiz, S. K. (2014). The effect of multi-scrolls distribution on image encryption. In *21st IEEE International Conference on Electronics, Circuits and Systems (ICECS), 2014* (pp. 435–438). IEEE.
49. Radwan, A. G., & Fouda, M. E. (2013). Optimization of fractional-order RLC filters. *Circuits, Systems, and Signal Processing*, 32(5), 2097–2118.
50. Radwan, A. G., Soliman, A. M., & El-Sedeek, A. L. (2003). An inductorless CMOS realization of Chua's circuit. *Chaos, Solitons & Fractals*, 18(1), 149–158.
51. Radwan, A. G., Elwakil, A. S., & Soliman, A. M. (2008a). Fractional-order sinusoidal oscillators: design procedure and practical examples. *IEEE Transactions on Circuits and Systems I: Regular Papers*, 55(7), 2051–2063.
52. Radwan, A. G., Soliman, A. M., & Elwakil, A. S. (2008b). First-order filters generalized to the fractional domain. *Journal of Circuits, Systems, and Computers*, 17(01), 55–66.
53. Radwan, A. G., Moaddy, K., & Momani, S. (2011a). Stability and non-standard finite difference method of the generalized Chua's circuit. *Computers & Mathematics with Applications*, 62(3), 961–970.
54. Radwan, A. G., Shamim, A., & Salama, K. N. (2011b). Theory of fractional order elements based impedance matching networks. *IEEE Microwave and Wireless Components Letters*, 21(3), 120–122.
55. Radwan, A. G., Abd-El-Hafiz, S. K., & AbdElHaleem, S. H. (2012). Image encryption in the fractional-order domain. In *International Conference on Engineering and Technology (ICET), 2012* (pp. 1–6). IEEE.
56. Radwan, A. G., Abd-El-Hafiz, S. K., & AbdElHaleem, S. H. (2014b). An image encryption system based on generalized discrete maps. In *21st IEEE International Conference on Electronics, Circuits and Systems (ICECS)* (pp. 283–286). IEEE.
57. Radwan, A. G., Abd-El-Hafiz, S. K., & AbdElHaleem, S. H. (2015a). Image encryption based on fractional-order chaotic generators. In *2015 International Symposium on Nonlinear Theory and its Applications NOLTA2015*, Kowloon, Hong Kong, China, 1–4 December 2015 (pp. 688–691). IEEE.
58. Radwan, A. G., AbdElHaleem, S. H., & Abd-El-Hafiz, S. K. (2015b). Symmetric encryption algorithms using chaotic and non-chaotic generators: A review. *Journal of Advanced Research*.
59. Sayed, W. S., Radwan, A. G., & Fahmy, H. A. (2015a). Design of a generalized bidirectional tent map suitable for encryption applications. In *2015 11th International Computer Engineering Conference (ICENCO)* (pp. 207–211). IEEE.
60. Sayed, W. S., Radwan, A. G., & Fahmy, H. A. H. (2015b). Design of positive, negative, and alternating sign generalized logistic maps. *Discrete Dynamics in Nature and Society*, 2015, Article ID 586783, 2015.
61. Sayed, W. S., Radwan, A. G., & Abd-El-Hafiez, S. K. (2016). Generalized synchronization involving a linear combination of fractional-order chaotic systems. In *13th International Conference on Electrical Engineering/Electronics, Computer, Telecommunications and Information Technology*.
62. Schöll, E. (2001). *Nonlinear spatio-temporal dynamics and chaos in semiconductors* (Vol. 10). Cambridge University Press.
63. Shamim, A., Radwan, A. G., & Salama, K. N. (2011). Fractional Smith chart theory. *IEEE Microwave and Wireless Components Letters*, 21(3), 117–119.

64. Soltan, A., Radwan, A. G., & Soliman, A. M. (2012). Fractional order filter with two fractional elements of dependant orders. *Microelectronics Journal*, 43(11), 818–827.
65. Sprott, J. C. (2000). A new class of chaotic circuit. *Physics Letters A*, 266(1), 19–23.
66. Srivastava, M., Ansari, S., Agrawal, S., Das, S., & Leung, A. (2014). Anti-synchronization between identical and non-identical fractional-order chaotic systems using active control method. *Nonlinear Dynamics*, 76(2), 905–914.
67. Strogatz, S. H. (2014). *Nonlinear dynamics and chaos: With applications to physics, biology, chemistry, and engineering*. Westview Press.
68. Vaidyanathan, S., & Azar, A. T. (2016a). Adaptive backstepping control and synchronization of a novel 3-D jerk system with an exponential nonlinearity. In *Advances in chaos theory and intelligent control* (pp. 249–274). Springer.
69. Vaidyanathan S, & Azar AT (2016b) Adaptive control and synchronization of Halvorsen circulant chaotic systems. In *Advances in chaos theory and intelligent control* (pp. 225–247). Springer.
70. Vaidyanathan, S., & Azar, A. T. (2016c). Dynamic analysis, adaptive feedback control and synchronization of an eight-term 3-D novel chaotic system with three quadratic nonlinearities. In *Advances in chaos theory and intelligent control* (pp. 155–178). Springer.
71. Vaidyanathan, S., & Azar, A. T. (2016d). Generalized projective synchronization of a novel hyperchaotic four-wing system via adaptive control method. In *Advances in chaos theory and intelligent control* (pp. 275–296). Springer.
72. Vaidyanathan, S., & Azar, A. T. (2016e). A novel 4-D four-wing chaotic system with four quadratic nonlinearities and its synchronization via adaptive control method. In *Advances in chaos theory and intelligent control* (pp. 203–224). Springer.
73. Vaidyanathan, S., & Azar, A. T. (2016f). Qualitative study and adaptive control of a novel 4-D hyperchaotic system with three quadratic nonlinearities. In *Advances in chaos theory and intelligent control* (pp. 179–202). Springer.
74. Vincent, U. (2008). Chaos synchronization using active control and backstepping control: A comparative analysis. *Nonlinear Analysis*, 13(2), 253–261.
75. Wedekind, I., & Parlitz, U. (2001). Experimental observation of synchronization and anti-synchronization of chaotic low-frequency-fluctuations in external cavity semiconductor lasers. *International Journal of Bifurcation and Chaos*, 11(04), 1141–1147.
76. Wu, X., Wang, H., & Lu, H. (2012). Modified generalized projective synchronization of a new fractional-order hyperchaotic system and its application to secure communication. *Nonlinear Analysis: Real World Applications*, 13(3), 1441–1450.
77. Yassen, M. T. (2005). Chaos synchronization between two different chaotic systems using active control. *Chaos, Solitons & Fractals*, 23(1), 131–140.
78. Yu, Y., & Li, H. X. (2008). The synchronization of fractional-order Rössler hyperchaotic systems. *Physica A: Statistical Mechanics and its Applications*, 387(5), 1393–1403.
79. Yuan, L. G., & Yang, Q. G. (2012). Parameter identification and synchronization of fractional-order chaotic systems. *Communications in Nonlinear Science and Numerical Simulation*, 17(1), 305–316.
80. Zidan, M. A., Radwan, A. G., & Salama, K. N. (2012). Controllable V-shape multiscroll butterfly attractor: System and circuit implementation. *International Journal of Bifurcation and Chaos*, 22(06), 1250,143.